Reactions at the Solid−Liquid Interface: Surface-Controlled Dissolution of Solid Particles. The Dissolution of Potassium Bicarbonate in Dimethylformamide

Claire L. Forryan,[†] Oleksiy V. Klymenko,[†] Colin M. Brennan,[‡] and Richard G. Compton*[,†]

Physical and Theoretical Chemistry Laboratory, University of Oxford, South Parks Road, Oxford OX1 3QZ, United Kingdom, and Syngenta, Leeds Road, Huddersfield HD2 1FF, United Kingdom

Received: July 26, 2004; In Final Form: November 1, 2004

We present a mathematical model for the surface-controlled dissolution of solid particles. This is applied to the dissolution of a solid having different particle size distribution functions: those of a monodispersed solid containing particles of all one size, a two-size-particle distribution, and a Gaussian distribution of the particle sizes. The dissolution of potassium bicarbonate in dimethylformamide is experimentally studied indirectly at elevated temperatures. We monitor the dissolution via the homogeneous deprotonation of 2-cyanophenol by dissolved $KHCO_3$. The loss of 2-cyanophenol was detected electrochemically at a platinum microdisk electrode, and separately, the formation of the 2-cyanophenolate anion was monitored via UV−visible spectroscopic analysis. The results presented show that the kinetics of the loss of 2-cyanophenol behaves on one hand as a homogeneous chemical process and on the other hand as a dissolution-rate-controlled process. Initially, predissolved $KHCO_3$ in solution deprotonates the 2-cyanophenol and homogeneous reaction dominates the observed kinetics, and at longer times, the observed kinetics is controlled by the rate of $KHCO_3$ dissolution. Modeling of the experimental results for the surface-controlled dissolution of $KHCO_3$ in dimethylformamide (DMF) yielded a mean value for the dissolution rate constant, k, at elevated temperatures; k was found to have a value of $(1.1 \pm 0.3) \times 10^{-8}$ mol cm^{-2} s^{-1} at 100 °C, and the activation energy for the dissolution was 34.4 ± 0.4 kJ mol^{-1} over the temperature range 60−100 °C.

1. Introduction

The dissolution of solid particles is of great importance in both industrial and natural processes.[1−11] Processes at the solid−liquid interface involve a coupled sequence of mass transport, adsorption/desorption phenomena, heterogeneous reaction, and chemical transfer of intermediates. Solid−liquid interfacial reactions may occur via several mechanisms:[12]

(1) The rate-determining step involves the dissolution of the solid substrate possibly followed by further reaction in the liquid phase.

(2) The reaction proceeds at the interface with the formation of soluble products.

(3) The reaction proceeds at or near the interface, forming insoluble products which may block further reaction.

(4) The reaction occurs within the (porous) solid.

In this paper, we focus our attention on the first mechanism listed above by investigating the dissolution kinetics of solid particles suspended in a solvent. In particular, we develop a theory for surface-controlled dissolution and illustrate this with reference to the dissolution of $KHCO_3$ in dimethylformamide (DMF).

Surprisingly, while heterogeneous solid/liquid systems are widely used in organic synthesis, there is little literature information on the dissolution of solid particles in organic solvents. Macfie et al. report the halogen exchange reaction of 2,4-dichloronitrobenzene with potassium fluoride in DMF.[13]

SCHEME 1: Scheme for the Reaction of Potassium Bicarbonate with 2-Cyanophenol in DMF

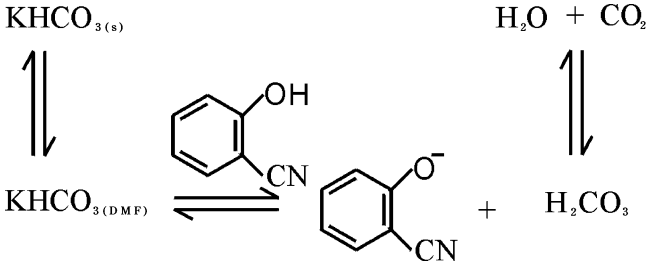

Their results show that, at longer times, the observed kinetics is controlled by the rate of KF dissolution; however, no kinetic information on this dissolution-rate-controlled process was obtained. The use of a strong base (e.g., potassium and sodium carbonates or potassium and sodium hydroxides) in an organic solvent (e.g., dimethylformamide, acetonitrile, or dimethyl sulfoxide) promotes many organic reactions such as epoxide synthesis from sulfur ylides,[14,15] synthesis of primary amines,[16,17] reduction of allylic nitro compounds to oximes,[16] and several alkylations.[15,18] Custers et al.[19] examined the tri-alkylation of methyl gallate; the reaction times appeared to be a function of the particle size distribution of the base, potassium carbonate. This prompted us to investigate the dissolution of solid particles in organic solvents by studying the dissolution of $KHCO_3$ in DMF. We monitor the dissolution via the homogeneous deprotonation of 2-cyanophenol by $KHCO_3$ in DMF at elevated temperatures; the $KHCO_3$ dissolves into the DMF solution, and it is this that deprotonates the 2-cyanophenol to form the 2-cyanophenolate anion, as shown in Scheme 1. Consequently, the loss of 2-cyanophenol and subsequent formation of the

* To whom correspondence should be addressed. Phone: +44-01865-275413. Fax: +44-01865-275410. E-mail: richard.compton@chemistry.ox.ac.uk.

[†] University of Oxford.

[‡] Syngenta.

10.1021/jp040508e CCC: $30.25
Published on Web 02/01/2005

2-cyanophenolate anion over time can provide information on the dissolution kinetics of $KHCO_3$.

We employed a real-time electrochemical method based on the voltammetric detection of 2-cyanophenol at a platinum microdisk electrode, combined with UV−visible spectroscopic analysis of samples removed from the reaction vessel. The solutions were heated via a heated microdisk method developed by Coles et al.,[20] which utilizes an electronically controlled heat gun that allows for greater precision in controlling the solution temperature. Power ultrasound was incorporated into the system to induce mixing, which has been shown to facilitate reproducible microelectrode responses in heterogeneous systems.[13]

The results show that over longer times the observed kinetics of the loss of 2-cyanophenol is controlled by the rate of dissolution of the inorganic solid. Initially, there is rapid deprotonation of 2-cyanophenol via predissolved solid in solution. Previously, the dissolutions of inorganic solids in acidic solutions, where the dissolution is via a reaction with H_3O^+ ions, have been successfully modeled[6,21,22] and the dissolution rate has been found to increase with decreasing particle size.[2−6,21] Thus far, these dissolutions as well as studies of the dissolution of limestone in aqueous electrolyte solutions[23−26] have been of selected particles of sizes in a small diameter fraction or single crystals, with the full particle size distribution of the inorganic solid not being considered.

We present a model for the surface-controlled dissolution of solid particles over time, as a function of the particle size distribution of the solid. The dissolutions are simulated for several theoretical particle size distributions: those of a monodispersed solid with particles of all one size, a two-size-particle distribution, and a Gaussian distribution of the particle sizes in the solid. The model is successfully applied to our experimental results to determine kinetic information on the dissolution of $KHCO_3$ in DMF at elevated temperatures.

2. Experimental Section

2.1. Chemical Reagents. All voltammetric experiments were carried out in *N*,*N*-dimethylformamide (DMF, Aldrich, 99.9+%, HPLC grade) with tetrabutylammonium perchlorate (TBAP, Fluka, puriss. electrochemical grade) as a supporting electrolyte. The DMF was carefully treated by drying over Linde 5 Å molecular sieves (Aldrich) for a minimum of 48 h, and then, prior to use, it was shaken with ICN alumina N-super 1 (ICN Biomedicals GmbH, Germany) and the solvent was decanted off. The water content of the solvent was determined by Karl Fischer titration (Metrohm, 758 KFD Titrino),[27] and it was found that the DMF drying procedure outlined above yielded DMF with a water content of ∼0.04 wt % (2.3×10^{-5} mol L^{-1}), compared to DMF as supplied, which has a water content of ∼0.15 wt % (8.6×10^{-5} mol L^{-1}).

2-Cyanophenol (Aldrich) and potassium bicarbonate (Aldrich) were obtained of the highest commercially available grade, and the potassium 2-cyanophenolate salt was supplied by Syngenta; all were used without further purification.

2.2. Instrumentation. *2.2.1. Electrochemical Measurements.* Cyclic voltammetry was recorded using a computer-controlled μAutolab potentiostat (Eco Chemie, The Netherlands) and carried out in a cell with a solution volume of 15 cm^3. A three-electrode design was employed consisting of a platinum counter electrode, a platinum pseudoreference electrode, and a platinum microdisk working electrode (radius 13.2 μm) manufactured in house according to a published procedure.[28] Prior to each electrochemical measurement, the microdisk electrode was polished on soft lapping pads (Kemet Ltd., U.K.) using alumina (Kemet Ltd., U.K.) of size 1 μm and 0.3 μm[7,29] and then rinsed in ultrapure water before carefully being dried and rinsed in the dried solvent. The electrode diameter of the microdisk was calibrated electrochemically using a 1 mM ferrocene solution in acetonitrile, containing 0.1 M TBAP, adopting a value for the diffusion coefficient of 2.3×10^{-5} cm^2 s^{-1} at 298 K.[30]

2.2.2. Heated Microdisk Cell and Ultrasound Setup. The ultrasonic generator used was a model VCX 5000 (Sonics and Materials, U.S.A.) horn equipped with a 3 mm diameter titanium microtip, emitting 25 kHz ultrasound. The power output of the transducer was calorimetrically calculated in DMF[31,32] for which an amplitude of 5% was found to correspond to 8 W cm^{-2} and was employed for all experiments.

The microelectrode high temperature experiments were carried out in a cell with a solution volume of 15 cm^3 by hot air circulation from an electronically controlled heat gun within a small box of insulating material with a front glass wall.[20] A Pt resistance thermometer controlled the air temperature, and a thermocouple in contact with the solution was used to read the temperature during the voltammetric scans. The platinum microdisk, reference, and counter electrodes and the utrasound horn were inserted from above into the cell, through precision bore apertures in the Teflon cell lid, which was manufactured in house to minimize heat losses. Temperature control was most important, and care was taken to ensure that all experiments were carried out at the required temperatures to ±1 °C. To maintain solution temperatures of 60, 80, 90, or 100 °C under the application of the power ultrasound, external heating from the heated microdisk setup required hot air circulation of approximately 55, 65, 80, and 86 °C, respectively.

The two regimes of inorganic solid and 2-cyanophenol addition that were adopted for this study were the following: (a) the 2-cyanophenol solutions in DMF/0.2 M TBAP were heated under ultrasound to the required elevated temperature, and upon stabilization of the temperature, the $KHCO_3$ was added, and (b) solutions of $KHCO_3$ in DMF/0.2 M TBAP were heated under ultrasound at elevated temperatures for a known time period (1−5 h) before the addition of 2-cyanophenol to the solution. The solutions were thoroughly degassed with nitrogen (BOC gases) throughout their initial heating, and a continuous flow of nitrogen over the solution was maintained throughout the electrochemical experiments to ensure that no oxygen was in contact. After the addition of either the inorganic solid (regime a) or the 2-cyanophenol (regime b), the platinum microdisk electrode was introduced into the cell and voltammetric scans were recorded at a scan rate of 50 mV s^{-1} 1 min after the addition and subsequently every 5 min for up to 1 h. Between each measurement, the electrode was removed and polished meticulously by the procedure outlined above.

2.2.3. UV−Visible Spectroscopy. UV−visible spectra were recorded on a Unicam UV2 series UV−visible spectrophotometer (Unicam, Cambridge, U.K.), using a quartz cuvette with a 1 cm path length, scanning over a wavelength of 275−400 nm. Small volume samples (∼100 μL) were removed at regular time intervals from the ultrasound-heated solutions, over a 1 h period, and allowed to cool to room temperature. These were diluted with DMF by a factor of 100 and their UV−visible spectra recorded. Each spectrum was background subtracted from that of blank DMF.

2.2.4. Particle Size Measurements. The particle size distribution was determined using a Malvern Mastersizer 2000 instrument (GLP no. 1345). The samples were analyzed in duplicate with dry powder 'Scirocco 2000' accessory using a measurement

time of 5 s, a background time of 5 s, a vibration feed rate of 60%, and a dispersive air pressure of 3 bar.

3. Theory

3.1. Surface-Controlled Dissolution of Solid Particles. In the kinetic treatment that follows, we consider the rate of the dissolution of solid particles, by modeling the number of moles of solid remaining undissolved in solution over time.

Let us consider a sample of particles of mass m and density ρ with the size distribution given by the distribution function $f(d)$, where d is the particle diameter. We assume that the particles are spherical and the volume of a single particle of diameter d_0 is

$$V_1(d_0) = \frac{\pi}{6} d_0^3 \tag{1}$$

and the number of moles of species in this particle is

$$n_1(d_0) = \frac{\pi}{6} d_0^3 \frac{\rho}{M} \tag{2}$$

where the subscript 1 indicates that the quantities are related to a single particle and M is the molecular weight of the species. After being placed into the solution, the particles start to dissolve with the rate constant k. The rate of change of the number of moles of the species in a particle is proportional to the rate constant, k, and the particle surface area, $S_1(d_0) = \pi d_0^2$. Hence, the following differential equation can be written for a single particle with the initial diameter d_0:

$$\frac{\mathrm{d}n_1(d_0, t)}{\mathrm{d}t} = -kS_1(d_0, t) = -\alpha n_1^{2/3}(d_0, t) \tag{3}$$

where $\alpha = k\pi^{1/3}(6M/\rho)^{2/3}$. The solution of this differential equation is given by

$$n_1(d_0, t) = \left[n_1^{1/3}(d_0, 0) - \frac{\alpha}{3}t\right]^3 \tag{4}$$

However, this expression gives negative values for $t > 3n_1^{1/3}(d_0, 0)/\alpha = d_0\rho/2kM$, that is, after a particle has been fully dissolved. Making use of the Heaviside step function, we can rewrite eq 4 as

$$n_1(d_0, t) = \left[n_1^{1/3}(d_0, 0) - \frac{\alpha}{3}t\right]^3 H\left(\frac{d_0\rho}{2kM} - t\right) \tag{5}$$

which is now correct for all values of t.

Consider now the number of particles with the initial diameter d_0. It is given by

$$\mathrm{d}N(d_0) = \frac{\mathrm{d}V(d_0)}{V_1(d_0)}$$

where $\mathrm{d}V(d_0)$ is the volume of all the particles of the size d_0 which is expressed as

$$\mathrm{d}V(d_0) = V f(d_0)\, \mathrm{d}d_0$$

where $V = m/\rho$ is the total mass of the particles and $V_1(d_0)$ is the volume of a single particle given in eq 1. Thus, we obtain the following expression for the number of particles

$$\mathrm{d}N(d_0) = \frac{6V}{\pi d_0^3} f(d_0)\, \mathrm{d}d_0 \tag{6}$$

Now, we can evaluate the number of moles in all particles that initially had the diameter d_0 as a function of time:

$$\mathrm{d}n(d_0, t) = n_1(d_0, t)\, \mathrm{d}N(d_0) = \left[n_1^{1/3}(d_0, 0) - \frac{\alpha}{3}t\right]^3 H\left(\frac{d_0\rho}{2kM} - t\right)\frac{6V}{\pi d_0^3} f(d_0)\, \mathrm{d}d_0 \tag{7}$$

Integrating eq 7 over all values of the particle diameter, we obtain the time dependence of the total number of moles of the species in the particle mixture:

$$n(t) = \frac{6V}{\pi}\int_0^\infty \left[n_1^{1/3}(d_0, 0) - \frac{\alpha}{3}t\right]^3 H\left(\frac{d_0\rho}{2kM} - t\right)\frac{f(d_0)}{d_0^3}\, \mathrm{d}d_0 \tag{8}$$

Note that due to the Heaviside function the integrand is exactly zero for the values of d_0 less than $2kMt/\rho$. Therefore, the Heaviside function can be eliminated from the integral by changing the integration limits which gives the final result in the form

$$n(t) = \frac{6m}{\pi\rho}\int_{\frac{2kM}{\rho}t}^\infty \left[\left(\frac{\pi\rho}{6M}\right)^{1/3} d_0 - \frac{\alpha}{3}t\right]^3 \frac{f(d_0)}{d_0^3}\, \mathrm{d}d_0 \tag{9}$$

Now we can evaluate eq 9 for different particle size distributions to obtain the time dependence of the number of moles of the solid in solution. For a monodispersed solid of which all particles are of the same size with the diameter a,

$$n(t) = \frac{6m}{\pi\rho a^3}\left[\left(\frac{\pi\rho}{6M}\right)^{1/3} a - \frac{\alpha}{3}t\right]^3 H\left(\frac{\rho a}{2kM} - t\right) \tag{10}$$

Next, we consider a sample of inorganic solid where there are particles of two different sizes with the diameters a_1 and a_2. The volume fraction of particles with diameter a_1 is given by γ, and the volume fraction of particles with diameter a_2 is therefore given by $1 - \gamma$. The expression for the particle size distribution function is

$$f(d) = \gamma\delta(a_1) + (1 - \gamma)\delta(a_2) \tag{11}$$

and upon solution of eq 9 gives

$$n(t) = \frac{6m}{\pi\rho}\left\{\frac{\gamma}{a_1^3}\left[\left(\frac{\pi\rho}{6M}\right)^{1/3} a_1 - \frac{\alpha}{3}t\right]^3 H\left(\frac{\rho a_1}{2kM} - t\right) + \frac{(1 - \gamma)}{a_2^3}\left[\left(\frac{\pi\rho}{6M}\right)^{1/3} a_2 - \frac{\alpha}{3}t\right]^3 H\left(\frac{\rho a_2}{2kM} - t\right)\right\} \tag{12}$$

For a Gaussian distribution function of particle sizes, where $\bar{a}$ is the mean particle diameter and σ is the standard deviation in diameter from the mean, the distribution function is given by

$$f(d) = \frac{1}{\sigma\sqrt{2\pi}} e^{(d-\bar{a})^2/2\sigma^2} \tag{13}$$

3.2. Theoretical Results. We investigated in turn the theoretical models presented above for the dissolution of a solid having monodispersed particles, a two-size-particle distribution and particle sizes of Gaussian distribution. In each case, the model is tested for a selected starting mass of solid, with k, the dissolution rate constant, having a value of 1.0×10^{-8} mol cm^{-2} s^{-1} corresponding to that determined below for the dissolution of $KHCO_3$ in DMF at 100 °C.

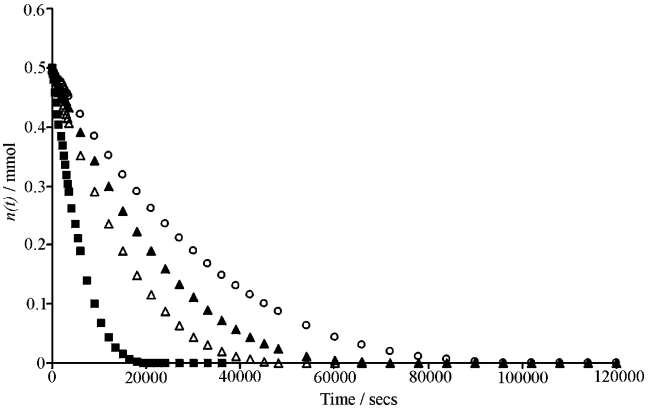

Figure 1. Plots of $n(t)$/mmol against time/s for the dissolution of 0.05 g of $KHCO_3$ containing particles with diameters of (■) 200 μm, (Δ) 500 μm, (▲) 700 μm, and (○) 1000 μm.

3.2.1. Monodispersed. For a starting mass of 0.05 g of $KHCO_3$ in solution, the dissolution with time was modeled for samples containing particles with diameters of 200, 500, 700, and 1000 μm. The resulting curves of the number of moles of undissolved $KHCO_3$, $n(t)$, against time are given in Figure 1. It can be seen that, as expected, the smaller the particle size, the more quickly they dissolve. The particles with larger diameters give a much slower loss of the solid into solution due to a smaller surface-to-volume ratio. For the particle sizes 200, 500, 700, and 1000 μm, the times taken to approach complete dissolution of $KHCO_3$ are 22 500, 60 000, 78 000, and 114 000 s, respectively. Hence, for faster dissolution of the inorganic solid, it is preferential for the solid to contain particles of the smallest size/diameter.

3.2.2. Two-Size-Particle Distribution. Let us consider a sample of $KHCO_3$ with a starting mass of 0.05 g in solution. The dissolution with time was modeled for samples containing particles of two sizes, the results of which are shown in Figure 2. In Figure 2a and b, there is primarily a rapid decrease in the number of moles of solid $KHCO_3$ in solution, which increases as the volume fraction of the smaller diameter particles increases. Thus, the dissolution of the smaller sized particles dominates over the initial time period. At longer times, the loss of solid $KHCO_3$ is a slower, gradual process, as the larger particles with a diameter of 700 μm dissolve in solution. In Figure 2c, the two particles are closer in size and the "two-curve" behavior seen in Figure 2a and b for the dissolution of small particles followed by that of the larger particles becomes less apparent. The dissolution curves converge as the two particle sizes become closer in diameter.

3.2.3. Gaussian Distribution. For a starting mass of 0.02 g of $KHCO_3$ in solution, the dissolution with time was modeled for samples having Gaussian distributions with $\bar{a} = 680$ μm and σ taking the values of 300, 200, 150, and 50 μm. The resulting curves of the number of moles of undissolved $KHCO_3$ against time are shown in Figure 3, all showing similar overall shapes. The insets in Figure 3 correspond to the enlargements of the curves over the initial and final time periods. Initially, the broader distribution functions give a faster dissolution of the solid, which appear linear over 10 000 s. Over time, the dissolution curves cross over; inset b shows that the sharper distribution of $\sigma = 50$ μm approaches complete dissolution of $KHCO_3$ more rapidly.

We compared the dissolution profiles for the Gaussian particle size distributions with that of a monodispersed sample of solid containing particles of size $\bar{a}$ as detailed on a separate plot, Figure 4. Taking particles of one size, the mean particle diameter, $\bar{a}$, gives a dissolution curve akin to those for the Gaussian distributions, with the behavior following more closely that of the sharper Gaussian distribution of $\sigma = 50$ μm, as expected with there being a greater volume fraction of particles of diameter $\bar{a}$. Hence, for a sample of solid with a particle size distribution function resembling that of the Gaussian type, the overall dissolution can be modeled approximately to that of a monodispersed solid.

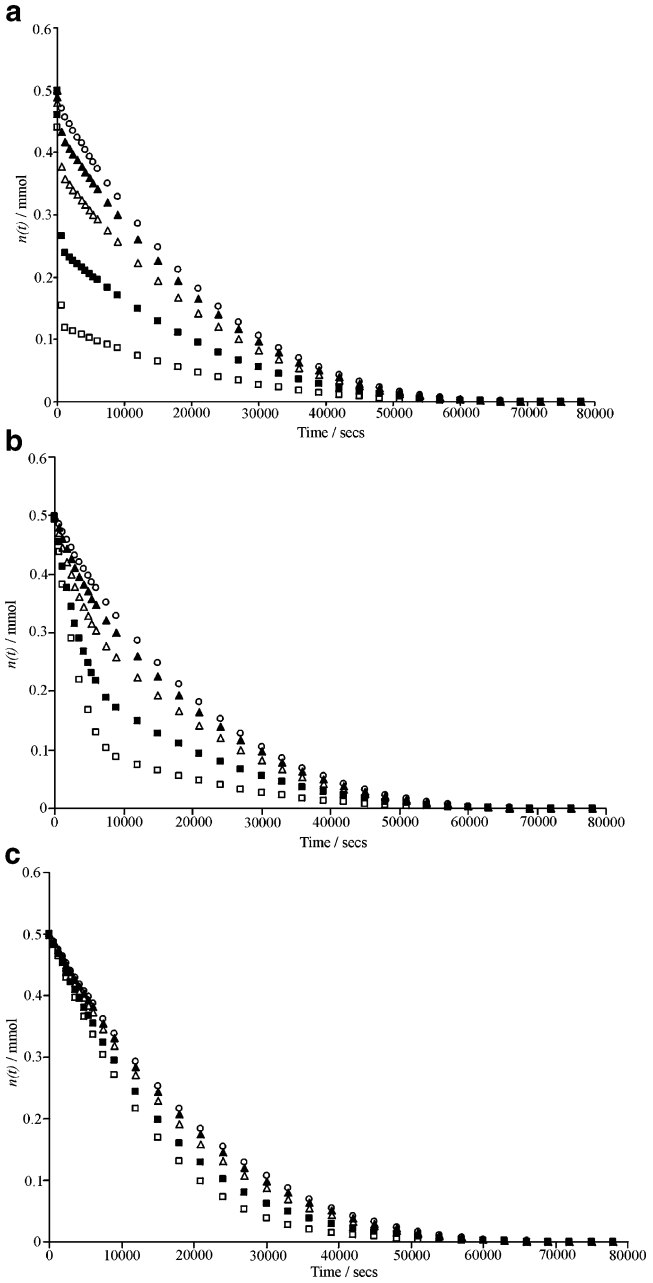

Figure 2. Plots of $n(t)$/mmol against time/s for the dissolution of 0.05 g of $KHCO_3$ with a two-size-particle distibution having (a) diameters of $a_1 = 10$ μm and $a_2 = 700$ μm, (b) diameters of $a_1 = 100$ μm and $a_2 = 700$ μm, and (c) diameters of $a_1 = 400$ μm and $a_2 = 700$ μm, with particle volume ratios, γ, of (○) 0.04, (▲) 0.125, (Δ) 0.25, (■) 0.5, and (□) 0.75.

4. Results and Discussion

4.1. Particle Size Distribution of $KHCO_3$. The particle size distribution function, $f(d)$, determined for a sample of the $KHCO_3$ used in all experiments is displayed in Figure 5. The mean particle diameter was calculated to be 679 ± 30 μm.

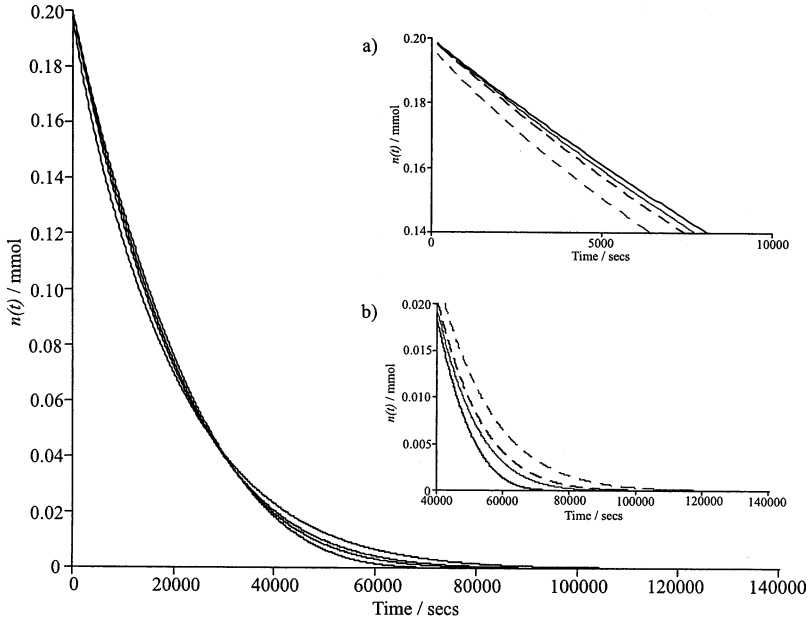

Figure 3. Plots of $n(t)$/mmol against time/s for the dissolution of 0.02 g of $KHCO_3$ with Gaussian particle size distribution functions with $\bar{a} = 680$ μm for σ values of (− − −) 300 μm, (— — —) 200 μm, (−) 150 μm, and (—) 50 μm. The inset shows enlarged portions of the graph for (a) 0−10 000 s and (b) 40 000−140 000 s.

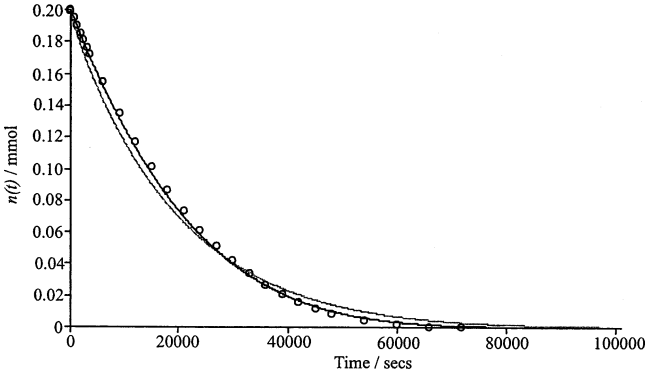

Figure 4. Plots of $n(t)$/mmol against time/s for the dissolution of 0.02 g of $KHCO_3$ containing particles of one size with diameters of (○) 680 μm and Gaussian particle size distribution functions with $\bar{a} = 680$ μm for σ values of (−) 300 μm and (—) 50 μm.

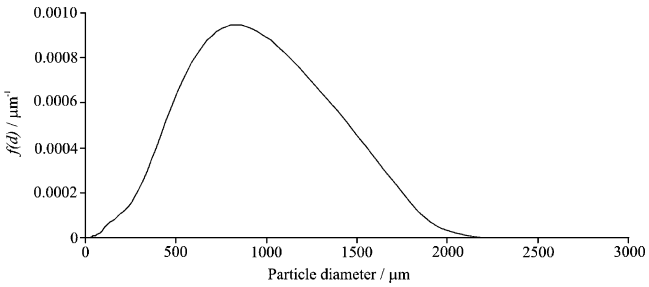

Figure 5. Particle size distribution for $KHCO_3$ used experimentally.

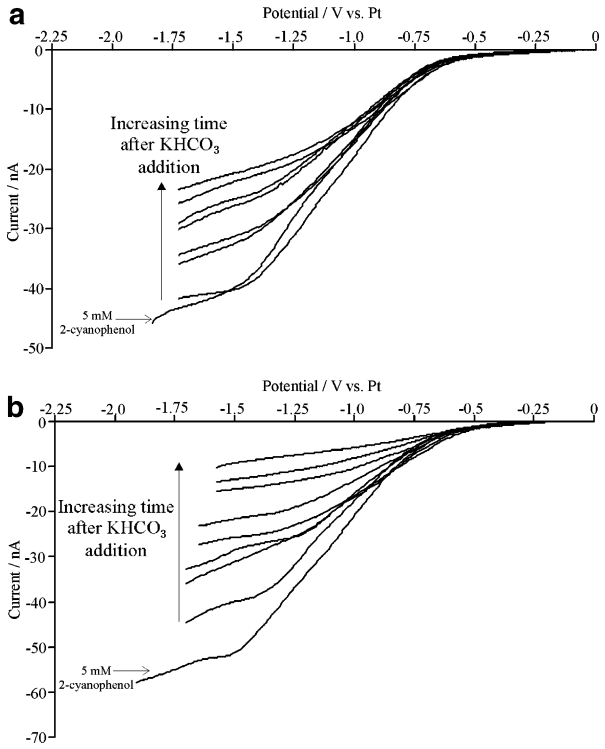

Figure 6. Steady-state voltammograms for the reductions at a platinum microdisk working electrode of a solution of 5 mM 2-cyanophenol in 0.2 M TBAP/DMF at temperatures of (a) 80 °C and (b) 100 °C, with the responses after the additions of 0.012 and 0.025 g of $KHCO_3$, respectively.

4.2. Electrochemical Results. Primarily, the electrochemical behavior of 2-cyanophenol in DMF and the response to the addition of $KHCO_3$ was investigated at elevated temperatures to develop a strategy for following the dissolution of $KHCO_3$ as the 2-cyanophenol "titrates" with the dissolved solid. The steady-state voltammetric responses for solutions of 5 mM 2-cyanophenol (0.2 M TBAP/DMF) at temperatures of 80 and 100 °C at a platinum microdisk electrode are detailed in parts a and b of Figure 6, respectively. These reveal one reduction wave for both temperatures of 80 and 100 °C at half potentials of −1.15 V versus Pt and −1.14 V versus Pt with limiting currents of 3.9×10^{-8} and 5.3×10^{-8} A, respectively. This wave can be attributed to the irreversible reduction of 2-cyanophenol to form the radical anion, which is consistent with previous studies of the reduction of 2-cyanophenol in DMF at room temperature[33] and elevated temperatures up to 100 °C[34] at gold microdisk electrodes. As shown in Scheme 2, the radical anion formed upon reduction is rapidly protonated by the parent molecule, the rate constant for which was found to be $\geq 1 \times 10^7$ M^{-1} s^{-1}, and hence, the net number of electrons per

SCHEME 2: Reaction Scheme for the Electrochemical Reduction of 2-Cyanophenol

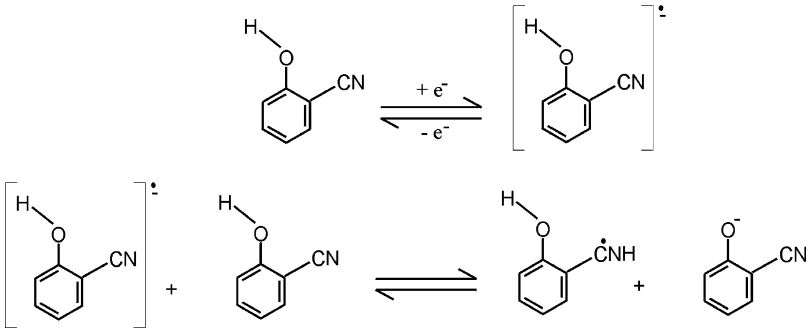

TABLE 1: Table of the Experimental Parameters Used in the Electrochemical Analysis

temperature/°C	mass of $KHCO_3$/g	[2-cyanophenol]/ mM	preheat ultrasound time/h	plots of limiting current against time
80	0.012, 0.025, 0.053, 0.111	5	N/A	Figure 7a
100	0.012, 0.025, 0.053, 0.111	5	N/A	Figure 7b
100	0.012, 0.025, 0.053, 0.111	5	3	Figure 8
80	0.025	5	1	Figure 9
80	0.025	5	3	Figure 9
80	0.025	5	4	Figure 9
80	0.025	5	5	Figure 9

cyanophenol reduced is approximately one-half.[33,34] Previously reported electron spin resonance (ESR) studies on 2-cyanophenol have given evidence that the protonated radical formed in Scheme 2 undergoes further reactions, generating other radical species.[35]

Solid $KHCO_3$ at a mass of 0.012 g was added to the 5 mM 2-cyanophenol solution at 80 °C, and 0.025 g of $KHCO_3$ was added to that at 100 °C. The voltammetric response for the 2-cyanophenol/radical anion reduction wave was measured 1 min after the addition and subsequently over a 1 h period, and the resulting responses are overlaid in parts a and b of Figure 6. Upon the addition of the solid, the half potential of the reduction wave shifts to less negative potentials of ~ -0.9 V versus Pt, indicative of a chemical reaction of the 2-cyanophenol. It can be seen at both temperatures that after the introduction of $KHCO_3$ to the solutions the limiting current for the reduction wave decreases over time. This corresponds to the deprotonation of 2-cyanophenol by $KHCO_3$ to form the 2-cyanophenolate anion, as depicted in Scheme 1. The decrease in limiting current corresponds to the loss of 2-cyanophenol from solution as it reacts over time with the $KHCO_3$. Hence, the deprotonation of 2-cyanophenol by the solid to form the 2-cyanophenolate anion can be monitored voltammetrically via analysis of the change in limiting current with time. It should be noted that the 2-cyanophenolate anion was found to be voltammetrically inactive in DMF; the electrochemical reduction of solutions of potassium 2-cyanophenolate in 0.2 M TBAP/DMF gave no responses at the platinum microdisk electrode.

Next, we investigated the deprotonation of 2-cyanophenol via dissolved $KHCO_3$ at elevated temperatures for the two regimes of inorganic solid and 2-cyanophenol additions: that where the 2-cyanophenol solutions were heated first and then $KHCO_3$ was added and that where the solutions of $KHCO_3$ in DMF were heated under ultrasound followed by 2-cyanophenol additions. From the voltammetric responses, the steady-state limiting currents were deduced by subtracting the observed limiting current from that of a blank background scan of 0.2 M TBAP/DMF at the elevated temperature concerned. These were plotted against time after the addition of the inorganic solid or 2-cyanophenol solutions. A table of the parameters for the individual experiments is given in Table 1.

As shown in Figure 7, the limiting current for each mass addition decreases over time, indicating the loss of 2-cyanophenol and the subsequent formation of the 2-cyanophenolate anion. UV−visible spectroscopic analysis of the starting solution and a sample of the solution at 100 °C taken 50 min after the addition of 0.053 g of $KHCO_3$ was performed to ascertain the extent of 2-cyanophenol consumption. The UV−visible spectrum of 0.05 mM 2-cyanophenol displayed one absorption peak at a wavenumber of 294 nm and an absorbance of 0.445. That of the reaction solution showed one peak at 358 nm with an absorbance of 0.472. The disappearance of the 2-cyanophenol peak indicates complete reaction of the 2-cyanophenol to form the phenolate. Furthermore, the reaction solution spectrum is comparable to that taken of a 0.1 mM solution of potassium 2-cyanophenolate, which exhibits a peak at 359 nm.[35] Hence, at 100 °C, the larger mass additions of 0.053 and 0.012 g of $KHCO_3$ give a loss of 2-cyanophenol with time as the 2-cyanophenolate anion is formed, with all the 2-cyanophenol being consumed after 50 min. The two smaller mass additions do not attain a total loss of the 5 mM 2-cyanophenol, as after 60 min the limiting current for 2-cyanophenol is detected at approximately one-half of its initial value. At 80 °C, the additions of $KHCO_3$ give a loss of 2-cyanophenol with time; the extent of the reaction increases with an increase in the mass of solid added, with the 0.111 g addition being the only one sufficient to give complete reaction. At both temperatures, the rate of 2-cyanophenol loss increases with an increase in the mass of $KHCO_3$ present, indicating the faster rate of 2-cyanophenolate formation with time.

A comparison between Figures 8 and 7b shows there is initially a much reduced limiting current for 2-cyanophenol and hence increased loss of 2-cyanophenol with pre-ultrasound of the $KHCO_3$/DMF solution. For the $KHCO_3$ masses of 0.012, 0.025, 0.053, and 0.111 g, after a reaction time of 1 min, there is an increase in the initial loss of 2-cyanophenol of 18, 35, 64, and 77%, respectively. These results suggest that the initial mechanism for 2-cyanophenol loss is via a homogeneous reaction with dissolved $KHCO_3$ in the DMF solution. For the higher mass of $KHCO_3$ of 0.111 g, it appears that, after applying ultrasound over a 3 h time period, there is sufficient dissolution of the inorganic solid in the DMF solution to give complete

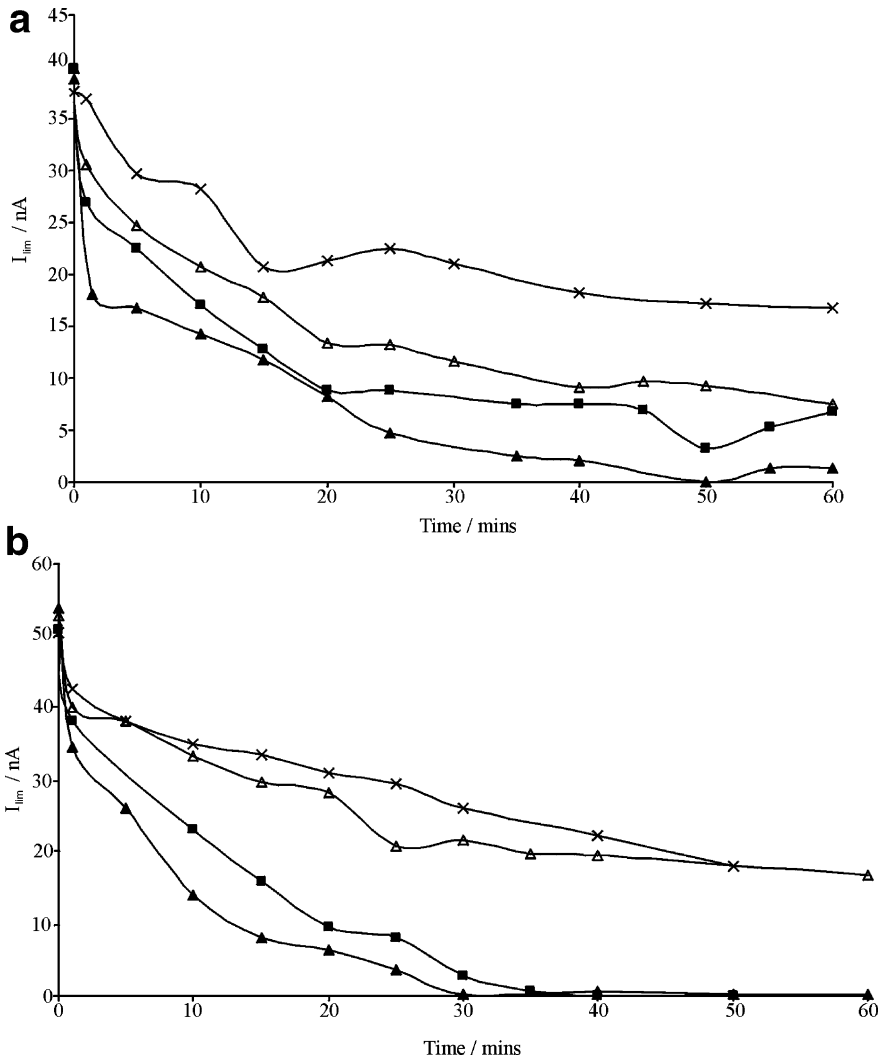

Figure 7. Plots of limiting current/nA against reaction time/min for a 5 mM solution of 2-cyanophenol in 0.2 M TBAP/DMF at (a) 80 °C and (b) 100 °C after the addition of (×) 0.012 g, (Δ) 0.025 g, (■) 0.053 g, and (▲) 0.111 g of $KHCO_3$.

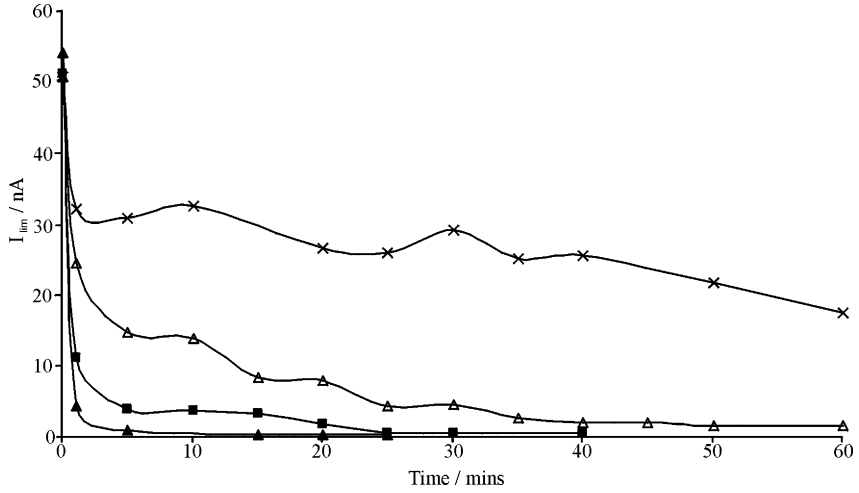

Figure 8. Plots of limiting current/nA against reaction time/min for (×) 0.012 g, (Δ) 0.025 g, (■) 0.053 g, and (▲) 0.111 g of $KHCO_3$ in 0.2 M TBAP/DMF heated under ultrasound at 100 °C for 3 h followed by the addition of 5 mM 2-cyanophenol.

reaction of the 2-cyanophenol to form the phenolate. For 0.012, 0.025, and 0.053 g of $KHCO_3$, after the initial rapid current decrease, at longer times, the limiting current of the 2-cyanophenol reduction wave decreases gradually, as observed in Figure 6b, showing a slow loss of 2-cyanophenol to form the phenolate. This implies that at longer times the loss of 2-cyanophenol is controlled by the rate of solid dissolution. The $KHCO_3$ dissolves in the DMF over time, and the 2-cyanophenol titrates with that released into the solution.

4.2.1. Effects of Ultrasound Time. The solubility of $KHCO_3$ in DMF is extremely low and known to be 0.8 ppm at room temperature;[36] no information is available on the solubility at elevated temperatures. Should the initial loss of 2-cyanophenol be via a homogeneous reaction of predissolved solid, it is

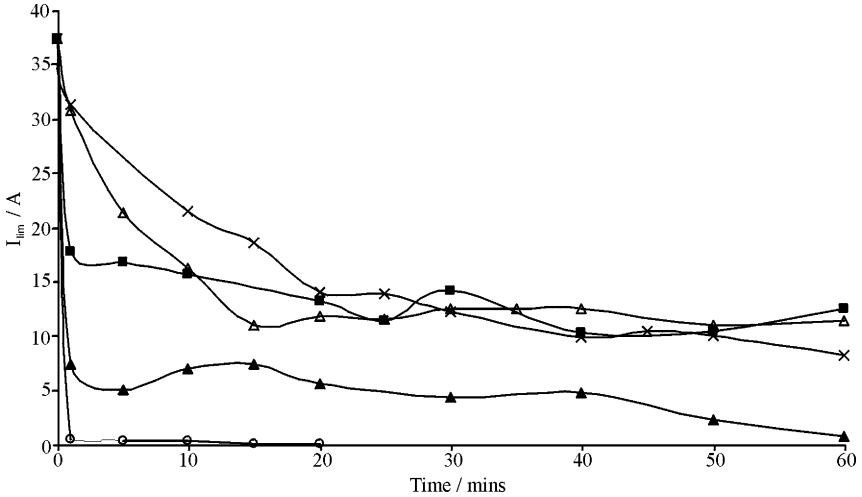

Figure 9. Plots of limiting current/nA against reaction time/min for the addition of 5 mM 2-cyanophenol to 0.025 g of $KHCO_3$ in 0.2 M TBAP/DMF heated under ultrasound at 80 °C for times of (×) 0 h, (Δ) 1 h, (■) 3 h, (▲) 4 h, and (○) 5 h.

TABLE 2: Table of the Experimental Parameters Used in the UV−Visible Spectroscopic Analysis

temperature/°C	mass of $KHCO_3$/g	[2-cyanophenol]/mM	preheat ultrasound time/h	k/mol cm^{-2} s^{-1}	plots of [2-cyanophenolate] against time
100	0.015	5	2	1.4×10^{-8}	Figure 10
100	0.020	5	2	1.1×10^{-8}	N/A
100	0.025	5	2	1.5×10^{-8}	10
100	0.030	5	2	1.2×10^{-8}	N/A
100	0.035	5	2	1.1×10^{-8}	Figure 10
100	0.008	1	2	8.6×10^{-9}	Figure 11
100	0.010	2	2	1.0×10^{-8}	N/A
100	0.050	10	2	1.6×10^{-8}	Figure 11
100	0.145	25	2	8.8×10^{-9}	N/A
100	0.250	50	2	8.4×10^{-9}	Figure 11
100	0.500	100	2	7.5×10^{-9}	Figure 11
80	0.035	5	2	5.2×10^{-9}	Figure 12
60	0.029	5	3	2.9×10^{-9}	Figure 12
90	0.029	5	2	7.6×10^{-9}	Figure 12
60	0.015	25	3	2.8×10^{-9}	Figure 12
90	0.015	25	2	7.9×10^{-9}	Figure 12

expected that this initial rate will be increased over longer dissolution times prior to 2-cyanophenol additions. To examine this, the $KHCO_3$/DMF solutions were heated and agitated under power ultrasound for increasing time periods to increase the initial dissolution of the solid; the experimental parameters are detailed in Table 1.

From Figure 9, it can clearly be seen that the initial rate of loss of 2-cyanophenol increases with pre-ultrasound time of the inorganic solid/DMF solutions. Ultrasound times of 1, 3, and 4 h show the initial homogeneous reaction of predissolved solid over 1 min. This is followed over longer times by the slow consumption of 2-cyanophenol as controlled by the rate of $KHCO_3$ dissolution. An ultrasound time period of 5 h gives sufficient dissolution of solid for all the 2-cyanophenol to react rapidly with the $KHCO_3$ already in solution, and consequently, the slower dissolution-controlled phase is not observed.

From the initial homogeneous reaction of predissolved solid, the loss in 2-cyanophenol over the first minute enabled the amounts of $KHCO_3$ dissolved in DMF after the various ultrasound times to be estimated. By using the following equation[37] for a microdisk electrode of radius r/cm, the concentration of unreacted 2-cyanophenol 1 min after solid addition was calculated from the steady-state limiting currents of the elevated temperature responses:

$$I_{lim} = 4nFDcr \tag{14}$$

The diffusion coefficient, D/cm^2 s^{-1}, was determined from an Arrhenius-type relation:

$$D = D_0 \exp(-E_A/RT) \tag{15}$$

where D_0/cm^2 s^{-1} is a constant, E_A/J mol^{-1} is the activation energy for the diffusion process, R is the molar gas constant (8.314 J K^{-1} mol^{-1}), and T/K is the temperature. We have previously reported values of D_0 and E_A for 2-cyanophenol of 5.1×10^{-3} cm^2 s^{-1} and 15.3 kJ mol^{-1}, respectively.[34] Taking a 1:1 mole ratio for the reaction of 2-cyanophenol with $KHCO_3$ (Scheme 1) allowed the determination of the number of moles of dissolved $KHCO_3$ which deprotonates the 2-cyanophenol. For the additions of 25 mg of $KHCO_3$ to 15 mL solutions of DMF, it was estimated that after ultrasound times of 1, 3, 4, and 5 h at a temperature of 80 °C the masses of $KHCO_3$ dissolved in solution were 1.8, 4.3, 6.2, and 7.5 mg, respectively.

4.3. UV−Visible Spectroscopic Analysis. The UV−visible spectrum of a 0.1 mM solution of potassium 2-cyanophenolate in DMF is known to display the phenolate absorption peak at 358 nm with an absorbance of 0.764.[35] The molar extiction coefficient, ϵ/mol L^{-1} cm^{-1}, for this peak was calculated by using the Beer−Lambert law.[38] This allows a further strategy for following the dissolution of $KHCO_3$, as dissolved solid deprotonates the 2-cyanophenol to produce the anion, which is detected spectroscopically. The absorbance of this peak was analyzed over reaction time for the addition of 2-cyanophenol to $KHCO_3$ solutions after predissolution ultrasound times of 2

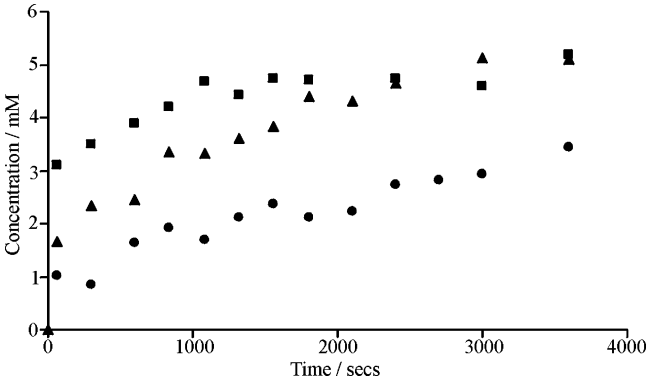

Figure 10. Plots of 2-cyanophenolate concentration/mM against reaction time/s for the addition of 5 mM 2-cyanophenol to (●) 0.015 g, (▲) 0.025 g, and (■) 0.035 g of $KHCO_3$ in DMF heated under ultrasound for 2 h at 100 °C.

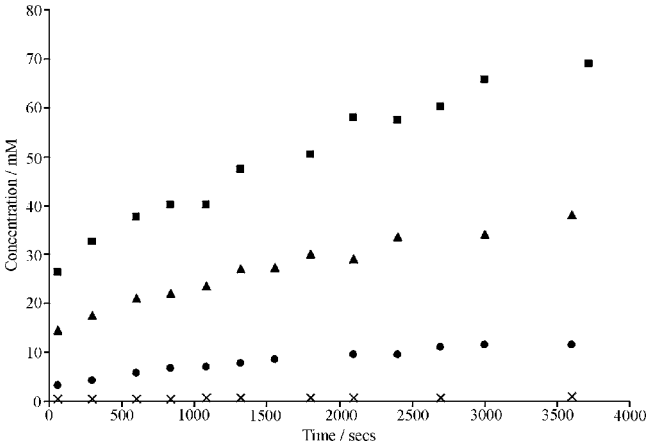

Figure 11. Plots of 2-cyanophenolate concentration/mM against reaction time/s for solutions of DMF with $KHCO_3$ heated under ultrasound for 2 h at 100 °C followed by the addition of 2-cyanophenol of concentrations of (×) 1 mM (0.008 g of $KHCO_3$), (●) 10 mM (0.050 g of $KHCO_3$), (▲) 50 mM (0.250 g of $KHCO_3$), and (■) 100 mM (0.500 g of $KHCO_3$).

h at elevated temperature. Table 2 details the parameters of individual experiments for varying masses of $KHCO_3$ and concentrations of 2-cyanophenol at 60, 80, 90, and 100 °C.

In Figure 10, as expected, there is an initial rapid formation of 2-cyanophenolate, due to reaction with predissolved solid. This is followed over longer times by a gradual increase in the 2-cyanophenolate produced. The 0.025 and 0.030 g additions form ∼5 mM phenolate after ∼2500 and ∼1800 s, respectively, indicating the complete reaction of the available 2-cyanophenol and hence no further production of the 2-cyanophenolate. The UV−visible results are consistent with those found voltammetrically.

Figure 11 details the results for varying concentrations of 2-cyanophenol additions. Over the entire concentration range, there is an initial rapid formation of 2-cyanophenolate; 0.45, 3.4, 14.6, and 26.4 mM 2-cyanophenolate was produced 1 min after the additions of 1, 10, 50, and 100 mM 2-cyanophenol, respectively, to the $KHCO_3$/DMF heated solutions. This is the homogeneous reaction of 2-cyanophenol with already dissolved $KHCO_3$ in the DMF solution. Over longer times, the gradual formation of the 2-cyanophenolate is again observed for all concentrations, with the loss of 2-cyanophenol being controlled by the rate of dissolution of solid $KHCO_3$ into the DMF solutions.

The addition of 2-cyanophenol to solutions of $KHCO_3$/DMF heated under ultrasound was examined for two further elevated

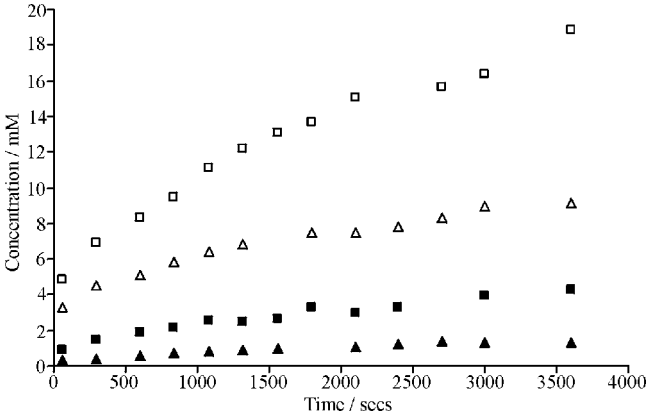

Figure 12. Plots of 2-cyanophenolate concentration/mM against reaction time/s for the addition of 5 mM 2-cyanophenol to 0.029 g of $KHCO_3$ in DMF at (▲) 60 °C and (■) 90 °C, and the addition of 25 mM 2-cyanophenol to 0.015 g of $KHCO_3$ in DMF at (Δ) 60 °C and (○) 90 °C, heated under ultrasound for 2 h.

temperatures of 60 and 90 °C, Figure 12. At each concentration, the initial homogeneous reaction of predissolved solid after 1 min gives an increased formation of 2-cyanophenolate at the higher temperature of 90 °C as compared to 60 °C, with the solubility of $KHCO_3$ being higher at 90 °C than at 60 °C. It can be seen that over longer times the rate of formation of 2-cyanophenolate is increased, with the gradients of the near linear concentration plots against time being higher at 90 °C than at 60 °C. Hence, the rate of dissolution of the $KHCO_3$ in DMF and reaction with 2-cyanophenol increases with increased temperature of the solution.

4.4. Modeling the Dissolution-Rate-Controlled Process. *4.4.1. Method.* The number of moles of solid $KHCO_3$ which remain undissolved in the solution at a given time were calculated from the voltammetric and UV−visible spectroscopic results as follows.

By using eqs 14 and 15, as described previously, the concentration of unreacted 2-cyanophenol at each reaction time was calculated from the steady-state limiting currents of the elevated temperature responses. Taking a 1:1 mole ratio for the reaction of 2-cyanophenol with $KHCO_3$ (Scheme 1) allowed the determination of dissolved $KHCO_3$ at each time. The starting number of moles for $KHCO_3$ was known from the mass of solid initially added, and hence, the number of moles of $KHCO_3$ remaining in solution at each time was calculated.

The concentration of 2-cyanophenolate formed at each reaction time in the UV−visible experiments was determined from the Beer−Lambert law, as described previously, and taking the 1:1 mole ratio of 2-cyanophenolate produced to $KHCO_3$ reacted, the number of moles of $KHCO_3$ remaining in solution at each time was calculated.

The solution to eq 9 was written in a program, incorporating the measured particle size distribution function for our sample of $KHCO_3$, to develop plots of the number of moles of undissolved inorganic solid, $n(t)$/mol, against the reaction time/s, where the following parameters were used: mass of the inorganic solid/g, density of the inorganic solid/g cm^{-3}, molecular weight of the inorganic solid/g mol^{-1}, time/s, k/mol cm^{-2} s^{-1}. As we are concerned with the dissolution-rate-controlled kinetics, the mass of solid used was calculated via subtraction of the mass predissolved in solution from the initial mass of solid added. Overlaying of plots of $n(t)$ against time for the theoretical model and the experimental data allowed values of k to be determined, as shown below.

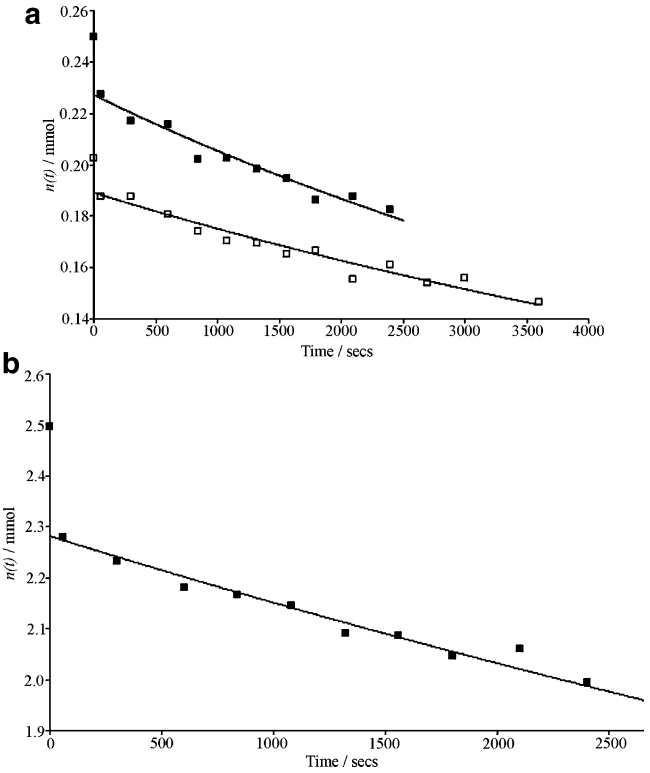

Figure 13. Plots of $n(t)$/mmol against time/s for theoretical (—) and UV−visible spectroscopic experimental results at 100 °C for the dissolution-rate-controlled process for (a) (■) 0.025 g of $KHCO_3$−5 mM 2-cyanophenol and (□) 0.020 g of $KHCO_3$−5 mM 2-cyanophenol and (b) (■) 0.250 g of $KHCO_3$−50 mM 2-cyanophenol.

4.4.2. Results. Initial results were gathered for the UV−visible experiments for the solutions of $KHCO_3$/DMF being heated at 100 °C under ultrasound for 2 h and then subsequent addition of the 2-cyanophenol. The first minute of reaction was not included in the fits, as this corresponds to the initial reaction of predissolved solid. Plots of $n(t)$ against time were performed over the $KHCO_3$ mass range of 0.015−0.035 g with additions of 5 mM 2-cyanophenol and with 2-cyanophenol of varying concentrations with known masses of $KHCO_3$. The optimum values of k found are tabulated in Table 2, while plots of the corresponding fit between experimental and theoretical data are shown in Figure 13. Good fits of theoretical to experimental data are seen. The mean value for the dissolution rate constant, k, for the dissolution of $KHCO_3$ in DMF and reaction with 2-cyanophenol at 100 °C is $(1.1 \pm 0.3) \times 10^{-8}$ mol cm^{-2} s^{-1}. The consistency of the dissolution rate constant at 100 °C provides strong evidence that over longer times the reaction of 2-cyanophenol with $KHCO_3$ is controlled by the rate of solid dissolution. Furthermore, the dissolution rate constant is independent of the concentration of 2-cyanophenol added and the initial mass of $KHCO_3$ present, hence supporting the dissolution model.

The voltammetric results for the 100 °C addition of 5 mM 2-cyanophenol to $KHCO_3$ in DMF/0.2 M TBAP show reasonable fits to the theoretical model. The k values obtained are in good agreement with those found from the UV−visible data, offering further evidence for the slow phase of 2-cyanophenol consumption being via a dissolution-controlled process.

Next, the effect of temperature on the dissolution-rate-controlled constant was examined. The UV−visible experimental results at 60, 80, and 90 °C were compared with the theoretical model and the plots detailed in Figure 14. The mean values of k determined from the best fits of theoretical to experimental data are $(2.9 \pm 0.1) \times 10^{-9}$ mol cm^{-2} s^{-1} at 60 °C, $(5.2 \pm 0.4) \times 10^{-9}$ mol cm^{-2} s^{-1} at 80 °C, and $(7.7 \pm 0.2) \times 10^{-9}$ mol cm^{-2} s^{-1} at 90 °C. A graph of ln k against $1/T$ over the temperature range 60−100 °C, inset of Figure 14, yields a straight line with an R^2 value of 0.9902. From the slope of the graph, the activation energy for the dissolution of $KHCO_3$ in DMF was calculated to be 34.4 ± 0.4 kJ mol^{-1}.

5. Conclusion

The dissolution of $KHCO_3$ in DMF at elevated temperatures was investigated by considering the deprotonation of 2-cyanophenol by dissolved $KHCO_3$ to form the 2-cyanophenolate anion, Scheme 1. The 2-cyanophenol titrates with the $KHCO_3$ that is released into solution upon its dissolution. Two independent experimental methods were employed to comprehensively study the dissolution process. The loss of 2-cyanophenol was detected voltammetrically via the decrease in limiting current for the steady-state response of 2-cyanophenol in DMF at the platinum microdisk electrode over time after the addition of $KHCO_3$. The formation of the 2-cyanophenolate anion was followed by UV−visible spectroscopic analysis. The results obtained show that the kinetics of the deprotonation of 2-cyano-

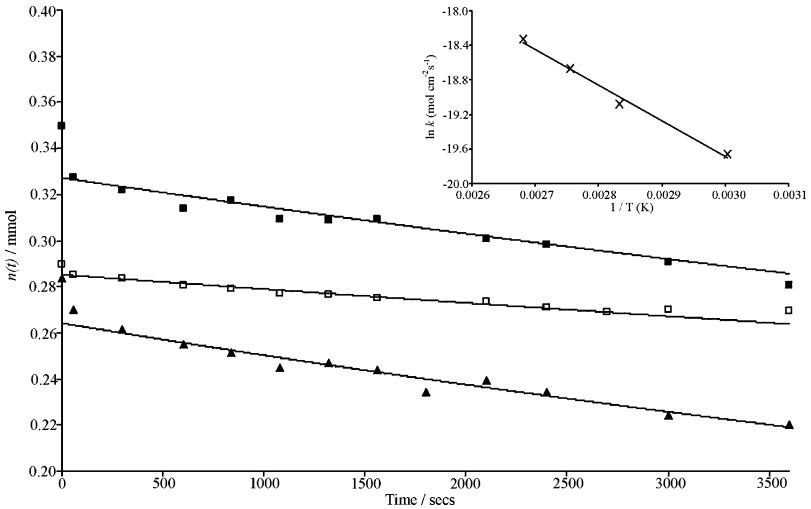

Figure 14. Plots of $n(t)$/mmol against time/s for theoretical (—) and UV−visible spectroscopic experimental results for the addition of 5 mM 2-cyanophenol to (□) 0.029 g of $KHCO_3$ in DMF at 60 °C, (■) 0.035 g of $KHCO_3$ in DMF at 80 °C, and (▲) 0.028 g of $KHCO_3$ in DMF at 90 °C. The inset shows a graph of ln(k/mol cm^{-2} s^{-1}) against 1/(T/K) over the temperature range 60−100 °C.

phenol with $KHCO_3$ in DMF exhibits varied kinetic behavior under different conditions. The initial kinetics for 2-cyanophenol deprotonation is a homogeneous reaction with predissolved $KHCO_3$ in the DMF solution, and at longer times, the observed kinetics is controlled by the rate of $KHCO_3$ dissolution.

We present a theoretical model for the surface-controlled dissolution of solid particles, in principle applicable to other solid/solvent systems where the particle size distribution of the solid is known. This model was employed to interpret the experimental results, and values for the dissolution rate constant, k, for the dissolution of $KHCO_3$ in DMF at elevated temperature were determined. It was found that k has a value of $(1.1 \pm 0.3) \times 10^{-8}$ mol cm^{-2} s^{-1} at 100 °C and that the activation energy for the dissolution was 34.4 ± 0.4 kJ mol^{-1} over the temperature range 60−100 °C.

Acknowledgment. C.L.F. expresses her gratitude to the EPSRC for a DTA studentship and Syngenta for a CASE award. We also thank Syngenta for carrying out the particle size measurements of $KHCO_3$, the preparation of the potassium 2-cyanophenolate salt, and the use of their facilities for carrying out the Karl Fischer titrations. O.V.K. thanks the Clarendon fund for partial support.

References and Notes

(1) Compton, R. G.; Harding, M. S.; Pluck, M. R. *J. Phys. Chem.* **1993**, *97*, 10416.
(2) Abali, Y.; Colak, S.; Yartaşi, A. *Hydrometallurgy* **1997**, *46*, 13.
(3) Özbek, H.; Abali, Y.; Colak, S.; Ceyhum, I.; Karagölge, Z. *Hydrometallurgy* **1999**, *51*, 173.
(4) Yartaşi, A.; Kocakerim, M. M.; Özmetin, C.; Abali, Y. *Miner. Eng.* **1996**, *9*, 1269.
(5) Yartaşi, A.; Kocakerim, M. M.; Yapıcı, S.; Özmetin, C. *Ind. Eng. Chem. Res.* **1994**, *33*, 2220.
(6) Künkül, A.; Demirkıran, N.; Baysar, A. *Ind. Eng. Chem. Res.* **2003**, *42*, 982.
(7) Welford, P. J.; Brookes, B. A.; Wadhawan, J. D.; McPeak, H. B.; Hahn, C. E. W.; Compton, R. G. *J. Phys. Chem. B* **2001**, *105*, 5253.
(8) Compton, R. G.; Daly, P. J. *J. Colloid Interface Sci.* **1984**, *101*, 159.
(9) Booth, J.; Sanders, G. S. H. W.; Compton, R. G.; Atherton, J. H.; Brennan, C. M. *J. Electroanal. Chem.* **1997**, *440*, 83.
(10) Sanders, G. S. H. W.; Booth, J.; Compton, R. G. *Langmuir* **1997**, *13*, 3.
(11) Tam, K. Y.; Compton, R. G.; Atherton, J. H.; Brennan, C. M.; Docherty, J. H. *J. Am. Chem. Soc.* **1996**, *118*, 4419.
(12) *Research in Chemical Kinetics*; Blackwell Science: Oxford, U.K., 1997; Vol. 4.
(13) Macfie, G.; Brookes, B. A.; Compton, R. G. *J. Phys. Chem. B* **2001**, *105*, 12534.
(14) Borredon, E.; Clavellinas, F.; Delmas, M.; Gaset, A.; Sinisterra, J. V. *J. Org. Chem.* **1990**, *55*, 501.
(15) Bentley, T. W.; Jones, R. V. H.; Larder, A. H.; Lock, S. J. *J. Chem. Soc., Chem. Commun.* **1994**, *19*, 2309.
(16) Albanese, D.; Landini, D.; Maia, A.; Penso, M. *J. Mol. Catal. A: Chem.* **1999**, *150*, 113.
(17) Landini, D.; Penso, M. *J. Org. Chem.* **1991**, *56*, 420.
(18) Fedorynski, M.; Wojciechowski, K.; Matacz, Z.; Makosza, M. *J. Org. Chem.* **1978**, *43*, 4682.
(19) Custers, J. P. A.; Hersmis, M. C.; Meuldijk, J.; Vekemans, J. A. J. M.; Hulshof, L. A. *Org. Process Res. Dev.* **2002**, *6*, 606−610.
(20) Moorcroft, M. J.; Lawrence, N. S.; Coles, B. A.; Compton, R. G.; Trevani, L. N. *J. Electroanal. Chem.* **2001**, *506*, 28.
(21) Temur, H.; Yartaşi, A.; Copur, M.; Kocakerim, M. M. *Ind. Eng. Chem. Res.* **2000**, *39*, 4114.
(22) Compton, R. G.; Pritchard, K. L.; Unwin, P. R. *Freshwater Biol.* **1989**, *22*, 285.
(23) Allers, T.; Luckas, M.; Schmidt, K. G. *Chem. Eng. Technol.* **2003**, *26*, 11.
(24) Allers, T.; Luckas, M.; Schmidt, K. G. *Chem. Eng. Technol.* **2003**, *26*, 12.
(25) Hong, Q.; Suárez, M. F.; Coles, B. A.; Compton, R. G. *J. Phys. Chem. B* **1997**, *101*, 5557.
(26) Wilkins, S. J.; Compton, R. G.; Viles, H. A. *J. Colloid Interface Sci.* **2001**, *242*, 378.
(27) Meyer, A. S., Jr.; Boyd, C. M. *Anal. Chem.* **1959**, *31*, 1.
(28) Wightman, R. M.; Wipf, D. O. *Electroanalytical Chemistry*; Bard, A. J., Ed.; Marcel Dekker: New York, 1989; Vol. 15.
(29) Cardwell, T. J.; Mocak, J.; Santos, J.; Bond, A. M. *Analyst* **1996**, *121*, 357.
(30) Sharp, P. *Electrochim. Acta* **1983**, *28*, 301.
(31) Margulis, M. A.; Mal'tsev, A. N. *Russ. J. Phys. Chem.* **1969**, *43*, 592.
(32) Banks, C. E.; Compton, R. G.; Fisher, A. C.; Henley, I. E. *Phys. Chem. Chem. Phys.* **2004**, *6*, 3147−3152.
(33) Forryan, C. L.; Lawrence, N. S.; Rees, N. V.; Compton, R. G. *J. Electroanal. Chem.* **2004**, *561*, 53.
(34) Forryan, C. L.; Compton, R. G. *Phys. Chem. Chem. Phys.* **2003**, *5*, 4226.
(35) Forryan, C. L.; Wain, A. J.; Brennan, C. M.; Compton, R. G. *Phys. Chem. Chem. Phys.* **2004**, *6*, 2989.
(36) As determined by Syngenta.
(37) Brett, C. M. A.; Brett, A. M. O. *Electrochemistry, Principles, Methods and Applications*; Oxford University Press: Oxford, U.K., 1993.
(38) Harwood, L. M.; Moody, C. J. *Experimental Organic Chemistry: Principles and Practice*; Blackwell Scientific Publications: Oxford, U.K., 1989.